EEP03

LPSC Grenoble, France, October 14-17, 2003

POLARIZATION OBSERVABLES IN THE $p(\vec{e}, e'\vec{p})\pi^0$ REACTION

Rikki E. Roché,
for the Hall A Collaboration

Department of Physics
Old Dominion University, Norfolk, VA 23529

The Thomas Jefferson National Accelerator Facility (Jefferson Lab) E91-011 ("$N \to \Delta$") experiment measured angular distributions of recoil polarization in the $p(\vec{e}, e'\vec{p})\pi^0$ reaction at $Q^2 \approx 1$ (GeV/c)^2 for a cm energy (W) near the Δ resonance, $1.16 \le W \le 1.36$ GeV. These data allowed for the extraction of 14 independent response functions along with two Rosenbluth combinations. By simultaneously fitting the angular distributions of these response functions, individual multipole amplitudes can be determined. This general multipole analysis is compared to representative models along with a traditional truncated Legendre analysis.

The "$N \to \Delta$" experiment was performed in Hall A of Jefferson Lab using a polarized electron beam of 4.53 GeV energy with an average beam current of 45 μA incident upon a 15 cm LH_2 target. The longitudinal polarization was monitored nearly continuously by a Compton polarimeter, measuring between 56 and 75%. Several comparison measurements were also made with a Møller polarimeter. Scattered electrons were detected in coincidence with recoil protons in the two Hall A high resolution spectrometers (HRS) with nominal acceptances of $\Delta\Omega = 6$ msr and $\Delta p/p = \pm 4\%$. The electron kinematics were fixed at $\theta_e = 14.1^\circ$ and a central momentum of $p_e = 3.7$ GeV/c at central values of $W = 1.232$ GeV and $Q^2 = 1.0$ (GeV/c)^2 with $\varepsilon \approx 0.95$. The proton kinematics varied over twelve settings covering the angular distribution for pion electroproduction. Because of the large acceptance of the HRS, considerable out-of-plane coverage was measured (see Fig. 1(a)).

The proton polarization at the focal plane was measured using a focal-plane polarimeter (FPP) with a carbon analyzer. A maximum-likelihood method was used to extract the target polarizations and response functions from the azimuthal distribution for scattering by the FPP analyzer. These target quantities were binned in $x = \cos\theta$, ϕ, W, and Q^2, as indicated by the solid lines in Fig. 1(a) and (b). Analysis details can be found in Refs. [1,2].

The differential cross section for pion electroproduction can be written as a

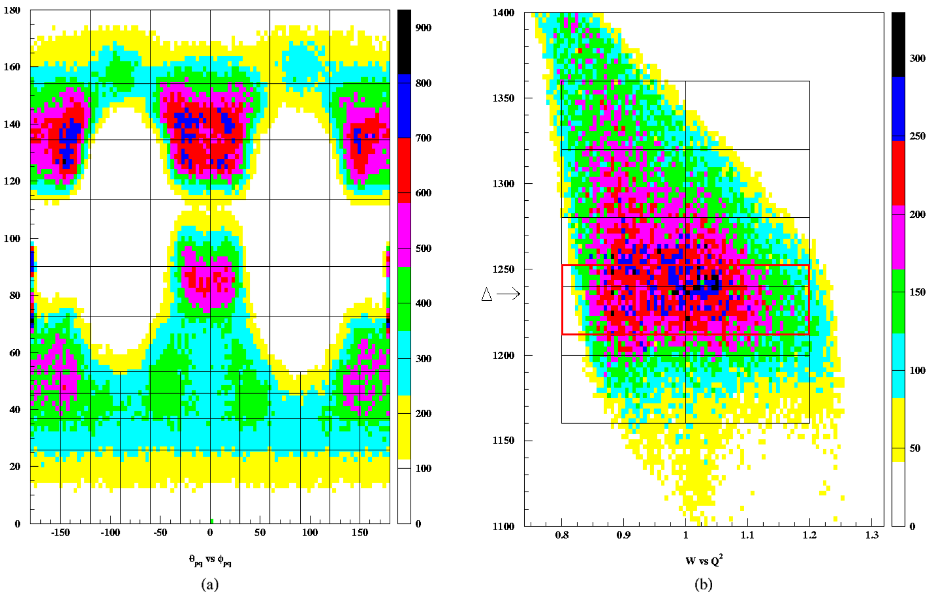

Figure 1: Kinematical acceptance and the binning used for polarization analysis: (a) angular acceptance for θ_N, ϕ_N in the cm frame, (b) W and Q^2 coverage. Solid lines correspond to binning used in data analysis.

combination of the physical observables, the proton polarization components[a]:

$$\frac{d^5\sigma}{dk_f d\Omega_e d\Omega^*} = \Gamma_\gamma \sigma_\circ \left[1 + hA + \vec{\Pi} \cdot \vec{S}\right], \tag{1}$$

where Γ_γ is the virtual photon flux of the initial (final) electron momenta k_i (k_f):

$$\Gamma_\gamma = \frac{\alpha}{2\pi^2} \frac{k_f}{k_i} \frac{k_\gamma}{Q^2} \frac{1}{1-\varepsilon}, \tag{2}$$

$k_\gamma = (W^2 - m_p^2)/2m_p$ is the laboratory energy a real photon would need to excite the same transition, $\varepsilon = (1 + 2\frac{\vec{q}^2}{Q^2} \tan^2 \frac{\theta_e}{2})^{-1}$ is the transverse polarization of the virtual photon, θ_e is the electron scattering angle, $\sigma_\circ$ is the unpolarized cross section, h is the electron helicity, A is the beam analyzing power, $\vec{\Pi} = \vec{P} + h\vec{P'}$ is the recoil proton polarization, and $\vec{S}$ is the spin direction of the recoil proton.

The polarization observables can be decomposed into products of kinematic factors, ν_α, and the response functions, $R_\alpha(x, W, Q^2)$, which carry the hadronic information:

$$\sigma_\circ = \nu_\circ \left(\nu_L R_L + \nu_T R_T + \nu_{LT} R_{LT} \cos\phi + \nu_{TT} R_{TT} \cos 2\phi\right), \tag{3}$$

[a] Electron kinematics and solid angle, $d\Omega_e$, are expressed in the lab frame; hadron kinematics and solid angle, $d\Omega^*$, are expressed in the πN center of mass frame.

$$A\sigma_\circ = \nu_\circ \left(\nu'_{LT} R'_{LT} \sin\phi\right), \tag{4}$$

$$P_n\sigma_\circ = \nu_\circ \left(\nu_L R^n_L + \nu_T R^n_T + \nu_{LT} R^n_{LT} \cos\phi + \nu_{TT} R^n_{TT} \cos 2\phi\right), \tag{5}$$

$$P_{l,t}\sigma_\circ = \nu_\circ \left(\nu_{LT} R^{l,t}_{LT} \sin\phi + \nu_{TT} R^{l,t}_{TT} \sin 2\phi\right), \tag{6}$$

$$P'_n\sigma_\circ = \nu_\circ \left(\nu'_{LT} R'^n_{LT} \sin\phi\right), \tag{7}$$

$$P'_{l,t}\sigma_\circ = \nu_\circ \left(\nu'_{LT} R'^{l,t}_{LT} \cos\phi + \nu'_{TT} R'^{l,t}_{TT}\right), \tag{8}$$

where the polarization vectors are expressed in a basis with $\widehat{l}$ along the nucleon momentum in the cm frame, $\widehat{n}$ normal to the reaction plane, and $\widehat{t} = \widehat{n} \times \widehat{l}$; $\nu_\circ = p_p/q_\circ$ is the ratio between the cm momentum in the final state and the cm momentum a real photon needs for the same transition, the kinematic factors describing the electron are defined as follows: $\nu_L = \varepsilon_s$, $\nu_T = 1$, $\nu_{LT} = \sqrt{2\varepsilon_s(1+\varepsilon)}$, $\nu_{TT} = \varepsilon$, $\nu'_{LT} = \sqrt{2\varepsilon_s(1-\varepsilon)}$, and $\nu'_{TT} = \sqrt{1-\varepsilon^2}$; and $\varepsilon_s = (Q^2/q^2)\varepsilon$ is the longitudinal polarization of the virtual photon.

Preliminary response function data for $(W, Q^2) = (1.232 \pm 0.02\ \text{GeV}, 1.0 \pm 0.2\ (\text{GeV/c})^2)$ are shown in Fig. 2. The twelve response functions shown in

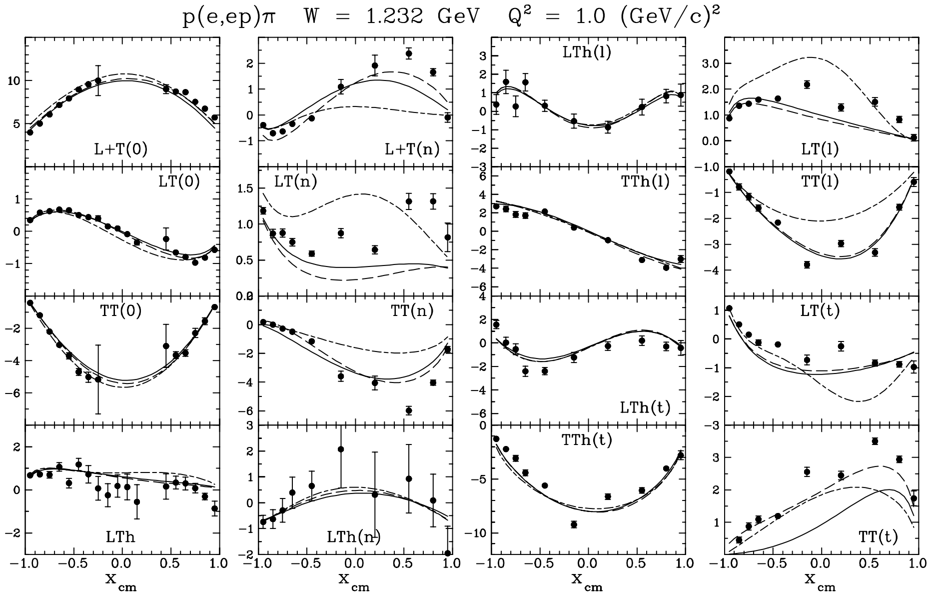

Figure 2: Response functions at $(W, Q^2) = (1.232\ \text{GeV}, 1.0\ (\text{GeV/c})^2)$ are compared with models: MAID2000 (solid), DMT (dashed), SAID (dash-dot). For each panel, the first part of the label describes the interference structure, inclusion of "*h*" indicates helicity dependence, and the recoil polarization is given in parentheses with "0" indicating an unpolarized response.

columns 2-4 have been measured for the first time in this experiment. Those shown in column three are dependent upon real parts of interference products and are dominated by the resonant amplitudes M_{1+}, E_{1+}, and S_{1+}. Those shown in columns two and four are dependent upon imaginary parts of interference products and are more sensitive to the non-resonant background amplitudes making model differences more pronounced. The data are compared to calculations based upon the MAID2000 [3], DMT [4], and SAID [5] models. None of these models is satisfactory in describing all of the extracted response functions.

By measuring a nearly complete set of recoil polarization response functions it becomes possible to perform a more general multipole analysis than the typically used Legendre expansion. In this multipole analysis the real or imaginary parts of one of the multipole amplitudes (M_{lj}, E_{lj}, or S_{lj}) can be represented as:

$$A\left(W,Q^2\right) = A^{(0)}\left(W,Q^2\right) + \delta A\left(W,Q^2\right) \tag{9}$$

where $A^{(0)}$ is the amplitude taken from a suitable model (eg. MAID or DMT) and δA is a correction to be fit to the data. By limiting the fit to variations of the s- and p-wave amplitudes, where all higher amplitudes are determined by the baseline model, there would be up to 14 free parameters for each (W, Q^2) bin to be fit to the (x, ϕ) distributions for the measured quantities (cross section, analyzing power, and helicity-dependent and helicity-independent recoil polarization components) simultaneously. The parameters to the x distributions of the 16 measured response functions could be fit instead. By including variations of the d-wave amplitudes the number of free parameters would be increased to 26 per (W, Q^2) bin while the sensitivity to the baseline model would be reduced.

Fig. 3 shows the fits for $(W, Q^2) = (1.232 \text{ GeV}, 1.0 \text{ (GeV/c)}^2)$ using this multipole analysis. The dashed lines correspond to a fit varying only s- and

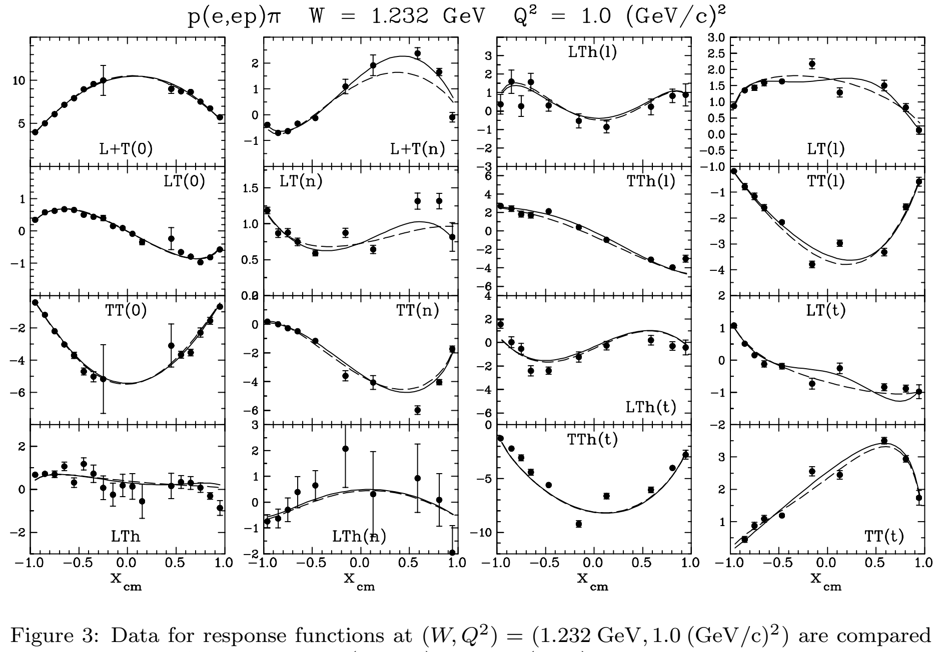

Figure 3: Data for response functions at $(W, Q^2) = (1.232 \text{ GeV}, 1.0 \text{ (GeV/c)}^2)$ are compared with fits that vary sp (dashed) and spd (solid) multipole amplitudes.

p-waves while the solid line is a fit varying d-wave amplitudes as well. The baseline model for both fits was MAID2000. There seems to be no systematic improvement in the fits by including variations in the d-wave amplitudes.

The typically quoted quadrupole deformation parameters EMR and CMR (or SMR) can be obtained directly from the fit multipole amplitudes. In Fig. 4, EMR and SMR determined directly from the multipole amplitudes are compared to the parameters found using the traditional method of a truncated Legendre expansion, details of which can be found in Ref. [6]. The multipole analysis

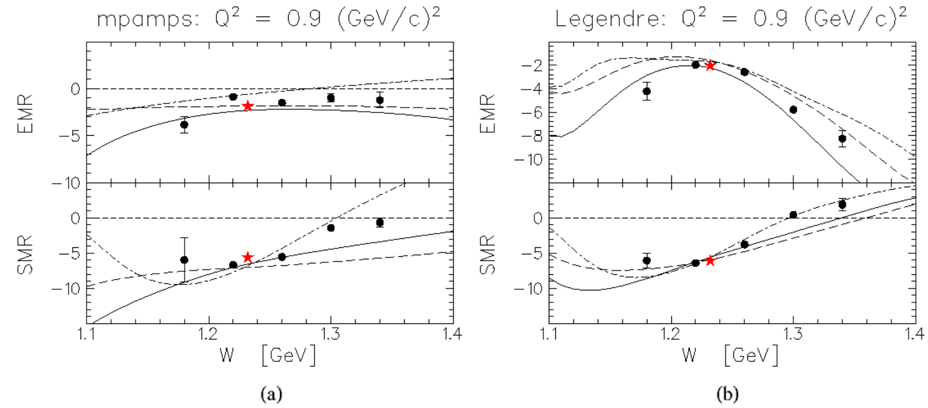

Figure 4: EMR and SMR data for $Q^2 = 0.9 \pm 0.1$ (GeV/c)^2 (black points) and $Q^2 = 1.0 \pm 0.2$ (GeV/c)^2 (red star) are compared with MAID2000 (solid), DMT (dashed), and SAID (dash-dot): (a) results from truncated Legendre expansion, (b) results from multipole analysis varying sp amplitudes with respect to MAID2000.

shows points determined using fits to s- and p- wave multipoles and MAID2000 as the baseline model. For SMR both methods show similar W dependencies over the measured range. The model calculations for SMR are in good agreement with the data near 1.232 GeV and describe the W dependence well, although MAID and DMT are in better agreement with each other than with SAID. For EMR, however, the two methods give different W dependencies and the model variation is greater. In the immediate vicinity of M_Δ these variations remain fairly small.

The Jefferson Lab Hall A "$N \to \Delta$" experiment measured angular distributions for recoil polarization in the $p(\vec{e}, e'\vec{p})\pi^0$ reaction at $Q^2 \approx 1$ (GeV/c)^2 with $1.16 \leq W \leq 1.36$ GeV across the Δ resonance. 14 independent response functions and two Rosenbluth combinations, 12 of which have been measured for the first time, have been obtained. Quantities dependent upon real parts of interference products differ little among models and agree relatively well with the data, while model differences and disagreements with data are much larger for quantities dependent upon imaginary parts which are more sensitive to non-resonant background amplitudes. A multipole analysis, where real and imaginary parts of multipoles for low partial waves are fit and higher non-resonant partial waves are constrained by models, has been compared to the traditionally used, less general truncated Legendre analysis to determine EMR and SMR for the $N \rightarrow \Delta$ transition. Good agreement and relatively little model dependence has been found between methods for SMR, while results for EMR seem to be more sensitive to the analysis method.

These results are still preliminary and should not yet be quoted. These results should be regarded as an indication of what should be possible with the final data. A more detailed presentation of the multipole amplitudes will be made in a later publication.

[1] R. E. Roché, Ph.D. thesis, Florida State University (2003).
[2] Z. Chai, Ph.D. thesis, Massachusetts Institute of Technology (2003).
[3] D. Drechsel *et al.*, *www.kph.uni-mainz.de/MAID*.
[4] D. Drechsel *et al.*, *www.kph.uni-mainz.de/MAID/dmt/dmt2001.html*.
[5] R. A. Arndt *et al.*, *gwdac.phys.gwu.edu*.
[6] J. J. Kelly, Proceedings of the conference on Nuclear and Particle Physics with CEBAF, Dubrovnik (2003).